We are IntechOpen, the world's leading publisher of Open Access books Built by scientists, for scientists

4,800
Open access books available

122,000
International authors and editors

135M
Downloads

Our authors are among the

154
Countries delivered to

TOP 1%
most cited scientists

12.2%
Contributors from top 500 universities

WEB OF SCIENCE™

Selection of our books indexed in the Book Citation Index in Web of Science™ Core Collection (BKCI)

Interested in publishing with us?
Contact book.department@intechopen.com

Numbers displayed above are based on latest data collected.
For more information visit www.intechopen.com

12

Synthesis and Luminescence Properties of $EuMoO_4$ Octahedron-Like Microcrystals

Jagannathan Thirumalai[1], Rathinam Chandramohan[2] and Viswanthan Saaminathan[3]
[1]*Department of Physics, B.S. Abdur Rahman University, Vandalur, Chennai, Tamil Nadu,*
[2]*Department of Physics,Sree Sevugan Annamalai College, Devakottai,Tamil Nadu*
[3]*School of Materials Science and Engineering, Nanyang Technical University, Singapore,*
[1,2]*India*
[3]*Singapore*

1. Introduction

Global claim for luminescent materials as efficient sources of energy that can supply sustained competence is growing day by day. The phosphors are facing increased challenges including concerns about global rare earth, environmental and recycling issues, and how to quickly bring to market new technological developments in the industry to meet end-user requirements. A number of applications have emerged in recent years that will change the future of the industry and new technologies like micro/nanoscale innovations and specialty phosphors are harnering increased attention. The primary drivers for growth are the expansion of key end-use applications including solid-state lighting and fluorescent lighting. Current research in nanotechnology is focused on new materials, novel phenomena, new characterization technique and fabrication of micro/nano devices.

Rare-earth doped molybdates are excellent materials of current interest owing to their interesting optical and opto-electronic properties. Scheelite-type crystalline structures, such as metal molybdates, where molybdenum atoms are coordinated tetrahedrally, have recently attracted great attention because of their promising applications in the electro-optical field (Ryu et al., 2005,a; Gong et al., 2006). Recently, molybdates have been extensively studied due to its attractive luminescence behavior and interesting structural properties (Thongtem et al., 2010), which can be used in a number of fields, such as optic fibers (Ryu et al., 2005, b) laser host materials (Wang et al., 2007), luminescence materials (Zhang et al., 2005; Sen & Pramanik, 2001), efficient catalysts (Ishii et al., 1992), scintillation detectors (Marques et al., 2006), and microwave application (Yang et al., 2009). Among all these molybdates, $EuMoO_4$ is an important opto-electrical material based on its red and white LED phosphors (Rosa et al., 2009). Furthermore, the molybdates allow the doping of different rare-earth ions, which can vary its luminescence properties. Due to the rich emission spectral lines extending from ultraviolet to infrared for Eu^{3+} ions, spectroscopic

properties of this ion have been extensively studied in various hosts to investigate the potential applications as functional material, in the fiber laser amplifiers, quantum cutting luminescence, up-conversion laser, and tunable ultraviolet (UV) , vacuum UV solid–solid-state lasers and High-pressure x-ray diffraction study (Errandonea et al., 2011; Koch et al., 1990; Zhang et al., 2007). New and enhanced properties are expected due to size confinement in nanoscale dimensions. In this background, this research work forms a recent avenue in material science research. The field of nanophosphor development, with rare earth doped metal oxide sytems have become a separate wide field in these days.

A detailed survey on undoped and doped molybdate phosphors discusses various synthesis techniques adopted by different research groups as follows. Recently, Eu^{3+} doped $ZnMoO_4$ with charge compensation were synthesized by solid-state reactions for phosphor-converted light-emitting diode (LED) is an important kind of solid-state illumination (Xie et al., 2010). Octahedron-like $BaMoO_4$ microcrystals were synthesized by the co-precipitation method at room temperature and processed in microwave-hydrothermal at 413 K for different time (Cavalcante et al., 2009). Single-crystalline $BaMoO_4$ microcrystals with uniform shuttle-like morphology have been successfully prepared via a facile aqueous solution mineralization process at room temperature (Wu et al., 2007). Phosphors $Na_5La(MoO_4)_4$:$x$$Eu^{3+}$ and $NaEu(MoO_4)_2$ were prepared with a solid-state reaction technique and are fabricated onto near-ultraviolet/violet-emitting InGaN chips for bright red-light-emitting diodes device, respectively (Wang et al., 2006). In order to prepare fluorescent material for white Light Emitting Diodes (LEDs), a new Eu^{3+} activated molybdate phosphor $SrMoO_4$ was fabricated with solid-state method (Xu et. al., 2007). Yttrium molybdate phosphors with fixed Er^{3+} and various Yb^{3+} concentrations were synthesized via a co-precipitation method (Lu et al., 2010). Tetragonal $La_2(MoO_4)_3$ with various novel and complex 3D hierarchical architectures self-assembled from different building blocks were successfully synthesized by a hydrothermal method in EDTA mediated processes (Xu et al., 2010). Enhancement emission intensity of $CaMoO_4$:Eu^{3+}, Na^+ phosphor via Bi co-doping and Si substitution for application to white LEDs phosphors were synthesized by the conventional solid state reaction method (Marques et al., 2008). $ZnMoO_4$ with a rhombus sheet or flower-like structure, α-$ZnMoO_4$ and needle-like $ZnMoO_4.0.8H_2O$ were successfully synthesized by simple hydrothermal crystallization processes with citric acid for opto-electronic applications (Zhang et al., 2010). The electronic structures of perfect crystals of barium molybdate (BaMoO4) and of crystals containing F and F+ color centers are studied within the framework of the fully relativistic self-consistent Dirac-Slater theory by using the numerically discrete variational (DV-Xα) method (Guo et al., 2009). Room temperature electrochemical growth of polycrystalline $BaMoO_4$ films on a metallic molybdenum substrate in a barium hydroxide aqueous solution has been studied (Xia & Fuenzalida, 2003). $BaMoO_4$ thin films were prepared on molybdenum substrates in $Ba(OH)_2$ solutions by electrochemical method at room temperature (Bi et al., 2003). Recently, on novel rare-earth activated molybdate [$K_xSr_{1-2x}MoO_4$:Pr^{3+}_x ($0.00 \le x \le 0.04$)] light-emitting diodes (LEDs) for the replacement of current light sources (Qiuxia et al., 2011). A novel red phosphor $Ca_{1-2x}Eu_xLi_xMoO_4$ is a promising material for Solid-State Lighting Based on a GaN LED (Wang et al., 2005). CaMoO4 was a promising yellowish green phosphor for near-ultraviolet (NUV) InGaN-based white LED (Li et al., 2007). Highly ordered $SrMoO_4$ 3D spherical superstructure assembled with nanosheets was synthesized via a facile and fast sonochemical route without any template (Mao et al., 2010). The indoor lighting applications are the main

potential applications using either white-light-emitting diode (LEDs) made by exciting appropriate phosphors. These wide band gap materials can be implemented commercially replacing all conventional LEDs in future. A well-crystallized AMO_4 (A=Ba, Ca, Sr; M=W, Mo) films have been prepared at room temperature through a simple solution reaction in respective alkaline solution at higher pH ~ 12–14 (Dinesh et al., 2005). X-ray diffraction and Raman scattering studies on the scheelite structured barium molybdate ($BaMoO_4$) under high pressure (~5.8 GPa) shows that, it undergoes a first order phase transition to the fergusonite structure ($I2/a$, $Z = 4$)—as also observed in iso-structural barium tungstate (Panchal et al., 2006). A study on the growth kinetics and habit modification of barium molybdate single crystals in silica gel medium has been presented (Kurien & Ittyachen, 1979). Praseodymium barium molybdate (PBM) single crystals grown by gel method, reveal multiple and isolated octahedral bipyramidal crystals as well as spherulites of PBM at different depths from the surface inside the gel (Isac et al., 1996). A series of novel red-emitting phosphors $AgLa_{0.95}Eu_{0.05}(WO_4)_{2-x}(MoO_4)_x$ [x=0–2] have been synthesized and their luminescence properties investigated (Sivakumar & Varadaraju, 2006). The effects of Ni^{2+} doping on structural, microstructural, dielectric and electrical properties of lead molybdate $PbMoO_3$ have been investigated. Ferroelectric phase transition in Ni-doped lead molybdate ceramics was studied (Palai et al., 2001).

Herein, we report the controlled synthesis of $EuMoO_4$ microcrystals using hydrothermal method by employing PVP as surfactant along with the state of the art of this field at present. By varying the reaction time, we have reported the morphology selection and the condition to derive octahedron morphology has been discussed. The rest of the parameters like, molar ratio between initial precursor / surfactant and temperature were kept as constant. The $EuMoO_4$ microcrystals are found to be an excellent matrix for photoluminescence application. The Eu^{3+} ion serves as a good red emitting luminescent center. Therefore, well-crystallized $EuMoO_4$ microcrystals have significant improvement in the phosphor properties considerably. Hence, the PL properties were also studied and reported. Also, this processing route provides the basis for a nearly low cost, low temperature method for the preparation of homogeneous nano-sized ceramics compared to any other existing methods.

2. Synthesis, structure, formation and morphology of the $EuMoO_4$ microcrystals

2.1 Synthesis

All the chemical reagents used were of analytical grade and used without further purification. In the typical synthesis, ~ 0.02 gm of PVP was first dissolved in 15 mL of deionized water under with vigorous stirring. Subsequently 0.021 mM of $(NH_4)_6Mo_7O_{24}\cdot 4H_2O$ was added drop wise. This is followed by addition of 1 mM $EuCl_2\cdot 7H_2O$ solutions drop wise to the above solution under with vigorous stirring by maintain the solution pH was adjusted up to 8. The mixture was stirred for another 10 min. Finally, the resultant solution was transferred to a Teflon-lined vessel kept in an autoclave at 135 °C for 0 – 7 hrs. The resultant solid products were centrifugally separated from the suspension, washed with deionized water and absolute ethanol several times, and dried at 60 °C in air for 6 hrs.

2.2 Structural analysis

The $BaMoO_4$ exhibit a scheelite-type tetragonal structure (Yang et al., 2008, Luo et al., 2009, Wu et al., 2007), which belongs to the tetragonal space group of $I4_1/a$. The unit-cell presents two formula units per primitive cell which includes two formula units where the Mo atom is surrounded by four equivalents O site in tetrahedral symmetry and divalent metal shares corners with eight adjacent MoO_4 tetrahedral [Luo et al., 2009, Ryu et al., 2005a]. Structure and phase purity of the $EuMoO_4$ microcrystals were examined using XRD analysis. From Fig. 1, it is seen that all the diffraction peaks matched well with the standard data for tetragonal scheelite-type $EuMoO_4$ (JCPDS, No. 22-1097; Space Group – $I4_1/a$). No traces of extra peaks from other phases were observed. Therefore, all as-prepared samples were of single phase $EuMoO_4$. The diffraction peaks (Fig. 1) are slightly broadened, which is characteristic of their fine nature. The average crystallite sizes of the primary particles that are calculated from peak broadening of the (112) line using the Scherrer formula was approximately 35 nm for $EuMoO_4$ microcrystals.

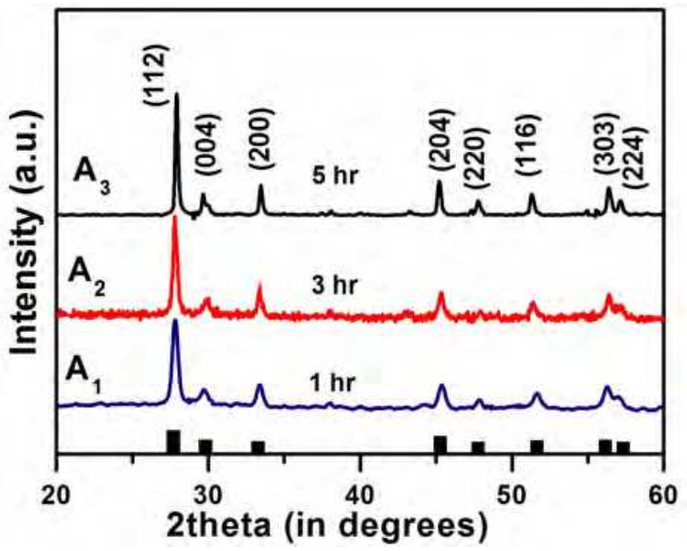

Fig. 1. X-ray diffraction (XRD) patterns of microstructures (A_1 – A_3) of $EuMoO_4$ prepared by modulating the reaction time (a) 1, (b) 3, (c) 5.

2.3 Morphological studies

The SEM and TEM images of the sample prepared with the typical procedure are shown in Fig 2. To obtain a better understanding of the formation mechanism of the $EuMoO_4$ octahedral-like microstructures, products formed at different growth stages were collected for SEM measurements. Fig 2 (a-e) implies that the concentration of PVP aqueous solutions played a crucial role in the formation of $EuMoO_4$ crystal prepared under various growth conditions. We found that the Ostwald ripening process dominated the crystal growth process at the initial stage. Fig. 2a shows some tiny equiaxial nanoparticles with polydisperse nature, at room temperature. As is well-known, at the initial stage tiny crystalline nuclei form in a supersaturated solution that acts as the nuclei for crystallization. Then the crystal growth follows, and bigger particles grow at the expense of smaller crystals, as described by the Gibbs-Thompson equation (Peng, 2003).

$$S_r = S_b \exp(2\sigma V_m / rRT) \quad (1)$$

where, *r*: is the radius of the crystal; *σ:* the specific surface energy; V_m*:* molar volume of the material; S_b *&* S_r*:* solubility of the bulk crystals and crystals with a radius *r,* respectively; *R,* the gas constant; *T,* the absolute temperature. Fig. 2b shows that the processing performed at 1h favoured the formation of bipyramidal-like microparticles to some extent agglomerated nature. By increasing the reaction time to 1 hr, the resulting product formation is due to the interactions between the tails of surface-adsorbed surfactant molecules, influencing the growth process of the micro-octahedrons. At ~ 3 hrs, it could be seen that $EuMoO_4$ octahedral microparticles of size ~ 1 μm side length were formed (Fig 2c), which is nearly similar to the structure of micro-octahedrons (Fig 2c). The growth rate in $EuMoO_4$ microcrystal is oriented preferentially along the [001] direction than in the [100] direction. In principle, we believe that the anisotropic growth in the [001] direction for the $EuMoO_4$ micro-octahedron is caused by differences in the surface energies on each crystal face. Probably, this preferential growth direction has stronger interatomic bonds between the $[Eu^{3+}]$ and $[MoO_4]^{2-}$ clusters. The microparticles synthesized with reaction time ~ 5 hrs are highly uniform, regular with smooth surface and can be dispersed well on a large scale. The PVP may form a complex the rare earth ions Pr^{3+} at first. Subsequently it might bind to the surface of the growing particles after being dissociated from the rare earth ions slowly in the process of reaction. Hence, the main factor to influence the formation of the regular structures is estimated as time. Formation of the octahedral-like $EuMoO_4$ microstructures after hydrothermal treatment are confirmed by TEM investigation. The corresponding high-resolution TEM image in Fig. 2d displays resolved lattice fringes of (004) planes with a spacing of 0.385 nm. Insets of Fig. 2(c, d) show the selected area electron diffraction (SAD). The Fast Fourier Transform (FFT) pattern indicates that the microstructures are single crystalline in nature. It is inferred that at the higher reaction time (Fig 2e), growth of the microcrystals lead to preferential growth orientation All together, from the SEM images, we can clearly see that microstructural changes occurred at the very early stages and even at lower reaction time. As reaction time was prolonged, only similar and much denser microcrystals could be grown.

2.4 Formation mechanism

The relevant formation mechanism of $EuMoO_4$ microstructures has been interpreted in two paths: dissolution–recrystallization and as well as the effective collision rates between the small microcrystals, respectively (Cavalcante et al., 2009, Luo et al., 2009). The hydrothermal process is able to promote the effective fender-bender between the small microparticles, contributing to the growth of the microcrystals and inducing the formation of new crystallographic faces on them. Schematic (Fig. 3) shows the morphological evolution of $EuMoO_4$ microcrystals as a function of reaction time. It is proposed that the process for the formation of the octahedron $EuMoO_4$ microcrystals. The first one is the formation of the perfect small microparticles, which belongs to a typical Ostwald ripening process. Probably, the preferential growth direction has stronger interatomic bonds between the $[Eu^{3+}]$ and $[MoO_4]^{2-}$ ions were mixed, a highly supersaturated solution was formed, leading to the coexistence of the asymmetrical and the bipyramidal-like $EuMoO_4$ microparticles. It is clear that the crystalline phase of the nuclei is critical for directing the inherent shapes of the crystals owing to its distinctive symmetry and structure. As the reaction time proceeded for 1 hrs, the bipyramidal-like particles are agglomerated with a high concentration of surface

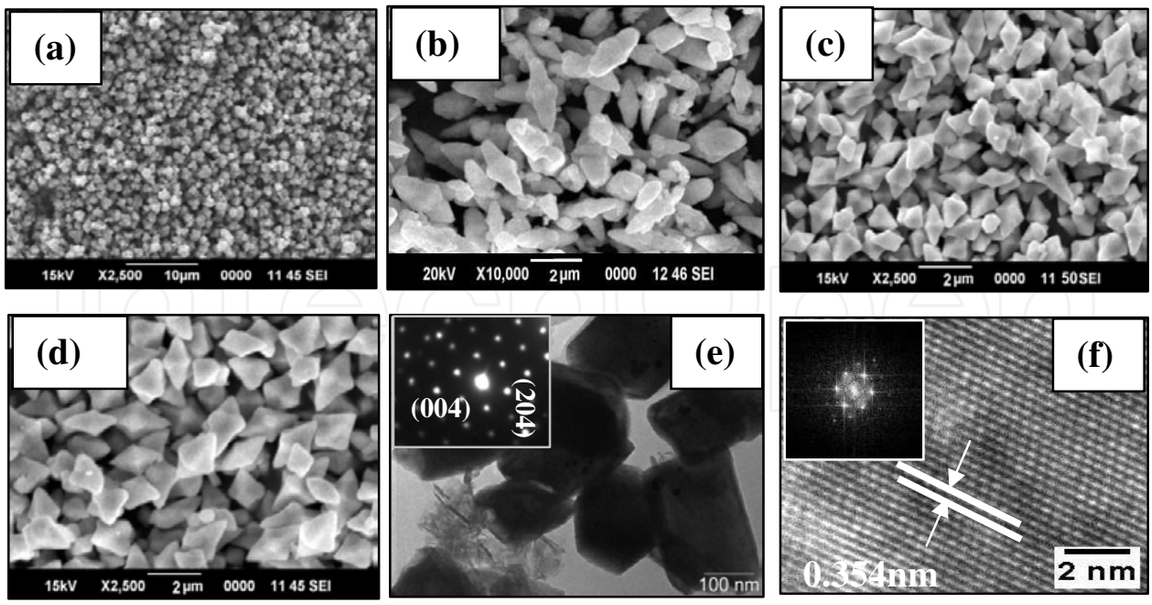

Fig. 2. Typical SEM image taken at different magnifications of $EuMoO_4$ microstructures at (a) Room temperature, (b) 1, (c) 3, (d) 5 hrs, (e) TEM image and the corresponding SAED pattern (inset) and (f) a typical HRTEM image and Inset: the corresponding FFT image.

defects and it is possible to note the initial formation of micro-octahedrons with well-defined structures. From 5 hrs of reaction time, the aggregation process between the small microparticles was induced by the coalescence process, resulting in the growth of micro-octahedrons. This proposed crystal growth mechanism is in good agreement with the literature (Cavalcante et al., 2009, Wu et al., 2007).

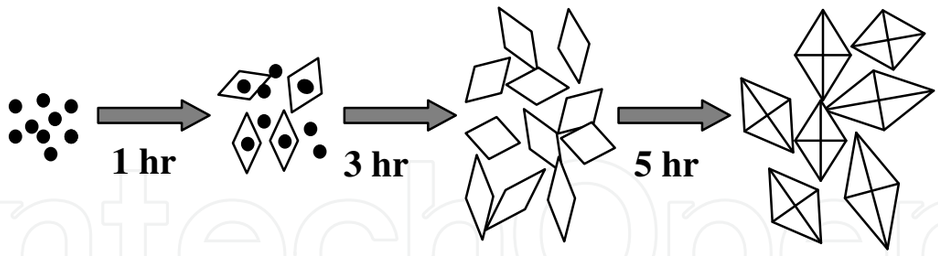

Fig. 3. Schematic representation of the formation process of the octahedron-like $EuMoO_4$ microcrystals.

2.5 Compositional analysis

It is well known that, the XPS is known to study the composition and binding energy. Therefore, in order to further prove that the as-synthesized $EuMoO_4$ microcrystals are composed of relevant elements. X-ray photoelectron spectroscopy (XPS) analysis was performed to probe the surface of the particles. The structures were probed using XPS, to investigate the elementary states and binding energy values. Fig. 4a shows the XPS survey spectra of the tetragonal $EuMoO_4$ microcrystals. The core levels of Eu, Mo and O can be seen in Fig. 2a, in which, the XPS spectra of the tetragonal $EuMoO_4$ microcrystals, obtained is the

range of 100 – 600 eV (Eu 4d at 130 eV, Mo $3d_{5/2}$ at 228.5 eV, Mo $3d_{3/2}$ at 331 eV, Mo $3p_{3/2}$ at 394 eV, Mo $3d_{1/2}$ at 412 eV, Mo 3s at 506 eV, O 1s 531.5 eV) and 1100 – 1200 eV (Eu $3d_{5/2}$ at 1126 eV, Eu $3d_{3/2}$ 1156.5 eV), respectively. It can be seen that the binding energy data (calibrated using C (1s, 284.7 eV) as the reference) from $EuMoO_4$ microparticles. All these peaks are in good agreement with the literature (Moulder, et al., 1992). The composition estimated by XPS using the relative sensitivity factors of Eu, Mo and O also revealed excess oxygen in the samples. The results also reveal that the sodium ions can be eliminated from the final product after washing and calcinations. The composition estimated using XPS results are in good agreement.

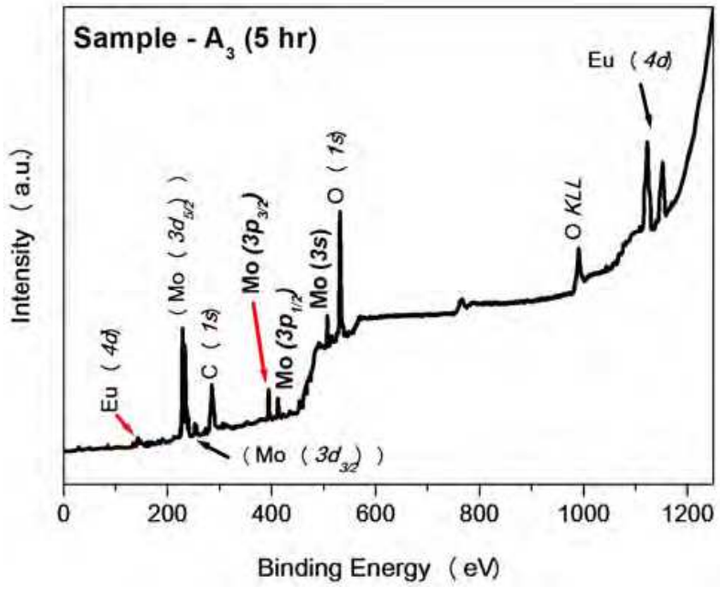

Fig. 4. XPS survey spectra of $EuMoO_4$ octahedron at 5 hr.

2.6 Optical properties

Fluorescence spectroscopy can provide valuable information about the intermolecular interactions of molecules in molecular crystals (Lifshitz, et al., 2003). The tetragonal phased $EuMoO_4$ has similar structure to that of other rare-earth doped molybdate ions with scheelite-type and is expected to be a promising phosphor candidate. The presence of strong clear peaks indicates the high crystallinity of the as-prepared products, which is very beneficial for obtaining brighter luminescence bands. The luminescence properties of the $EuMoO_4$ phosphors were then examined. Fig. 5 presents the excitation and emission spectra of $EuMoO_4$ microstructures.

The excitation spectra (Fig. 5, left) were obtained by monitoring the emission of the Eu^{3+} $^5D_0 \rightarrow {}^7F_2$ transition at 616 nm. It can be observed clearly that the excitation spectra both consist of a broadband from 200 to 350 nm, which is ascribed to the O—Mo C–T transition. The C–T band of O—Eu^{3+}, which usually appears in the range of 250–300nm in the excitation spectrum (Kiselev, et al., 2008), might have overlapped with the C–T band of molybdate group and, hence, as not observed clearly. In the longer wavelength region (360–710 nm), the sharp lines are intraconfigurational *4f–4f* transitions of Eu^{3+} in the host lattices, and the

strong excitation band at 395 and 465nm is attributed to the $^7F_0 \rightarrow ^5L_6$ and $^7F_0 \rightarrow ^5D_2$ transitions of Eu^{3+}, respectively. The emission spectra of Eu^{3+} (Fig. 5, right) excited under 395nm near-UV light are mainly dominated by the hypersensitive red emission, showing a strong transition $^5D_0 \rightarrow ^7F_2$ at 616nm and a weak $^5D_0 \rightarrow ^7F_1$ transition. The two peaks are assigned to the electric dipole transition and magnetic dipole transition, respectively, and the presence of electric dipole transition confirms that Eu^{3+} ions are located at sites without inversion symmetry. From the PL emission spectra it is clearly attrributed that the transition from its major lines is greatly enhanced, and thus a bright red emission is observed. Since the absorption / emission process depends strongly on the nature of the lattice and its constituents, the luminescence behaviour of Eu^{3+} compounds is expected to vary strongly with the preparatory conditions. This is what has been observed. The strong luminescence intensity indicated the perfection of the microstructure and good crystallization. The optical property of the $EuMoO_4$ are in good agreement with the literature (Kiselev, et al., 2008), that were obtained by solid-state reaction method. The trivalent europium ion (Eu^{3+}) in solids has an intricate energy level scheme with energy gaps of various magnitude and show rich emission spectral lines (Blasse & Grabmaier, 1994). Also a systematic study related to PL and the lifetime measurements are to be undertaken. Such photoluminescent materials have potential application and an efficient red phosphor candidate in the luminescence field. The result envisages an effective route to synthesize $EuMoO_4$ microstructures have potential application in biomedical and display systems.

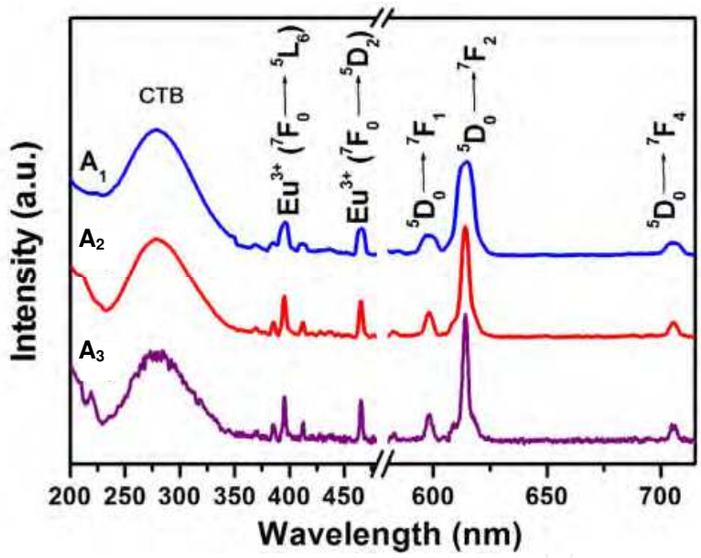

Fig. 5. A part of room temperature PL of $EuMoO_4$ microstructures (A_1 – A_3): excitation spectra (monitored at 643 nm) and emission spectra (under 443 nm excitation) prepared by modulating the reaction time.

In summary, this novel $EuMoO_4$ microstructures have been successfully synthesized via a facile simple and mild hydrothermal route employing PVP as surfactant. It is interesting to observe that the microparticles are highly crystalline and with uniform octahedral-like morphology in size and shape. The use of PVP as a surfactant introduced into the reaction system is essential to obtain highly crystalline and smooth surface microparticles. A strong red emission centered at 643 nm corresponding to the $^3P_0 \rightarrow ^3F_2$ transition of Eu^{3+} is

observed under 440 – 500 nm excitation. The grown $EuMoO_4$ microstructures showed strong red emission upon UV illumination, finds potential application in biomedical and display devices. Altogether, this preparation methodology is found to be highly reproducible, convenient, easy, and could be extended to prepare other rare-earth doped molybdate microstructures for various applications like electroluminescent devices, optical integrated circuits, or biomarkers.

3. References

Bi, J.; Xiao, D. Q.; Gao, D. J.; Yu, P.; Yu, G. L.; Zhang, W. & Zhu, J. G. (2003). $BaMoO_4$ thin films prepared by electrochemical method at room temperature Cryst. Res. & Tech., 38., 11., (October & 2003) 935–940, ISSN: 0232-1300.

Blasse, G. & Grabmaier B.C. (1994). Luminescent Materials, Springer-Verlag Telos, 1-232, ISBN: 0387580190, New York.

Cavalcante, L. S.; Sczancoski, J. C.; Tranquilin, R. L.; Varela, J. A.; Longo, E. & Orlandi, M. O. (2009). Growth mechanism of octahedron-like BaMoO4 microcrystals processed in microwave-hydrothermal: Experimental observations and computational modeling. *Particuology*, 7., 5., (May & 2009) 353 – 362, ISSN: 1674-2001.

Dinesh, R.; Fujiwara, T.; Watanabe, T.; Byrappa, K. & Yoshimura, M. (2005). Solution synthesis of crystallized AMO_4 (A=Ba, Sr, Ca; M=W, Mo) film at room temperature. *J. Mater. Sci.* 41., 5., (March & 2005) 1541-1546, ISSN: 0022-2461.

Errandonea, D.; Santamaria-Perez, D.; Achary, S. N.; Tyagi, A. K.; Gall, P. & Gougeon, P. (2011). High-pressure x-ray diffraction study of CdMoO4 and EuMoO4, *J. Appl. Phys.* 109, February 2011) 043510–5, ISSN: 0021- 8979.

Gong, Q.; Qian, X.; Cao, H.; Du, W.; Ma, X. & Mo, M. (2006). Novel Shape Evolution of $BaMoO_4$ Microcrystals. *J. Phys. Chem. B.* 110., 39., (September & 2006) 19295–19299, ISSN: 1520-6106.

Guo, X.; Zhang, Q., Liu, T.; Song, M.; Yin, J.; Zhang, H. & Wang, X. (2009). First-principles study on electronic structures of $BaMoO_4$ crystals containing F and F^+ color centers. *Nuc. Inst. Methods. Phys. Res.: Sec. B*. 267., 7., (April & 2009) 1093–1096, ISSN: 0168-583X.

Isac, J.; Ittyachen, M. A. & Raju, K. S. (1996). Praseodymium barium molybdate-its growth and structural characterization *Bull. Mater. Sci.* 19., 3., (October & 1995) 495-504, ISSN: 0250-4707.

Ishii, M. & Kobayashi, M. (1992). Single crystals for radiation detectors. *Prog. Cryst. Growth Charact. Mater.* 23., 7-8., (August& 1991) 245–311, ISSN: 0960-8974.

Kiselev, A. P.; Shmurak, S. Z.; Sinitsyn, V. V.; Khasanov, S. S.; Red'kin, B. S.; Alekseev, A. V. & Ponyatovskii, E. G. (2008). Spectroscopy and X-Ray Diffraction Analysis of Europium Molybdate Single Crystals Subjected to Different Thermobaric Treatments, *Bull. Russian Academy Sci.: Physics,* 72., 9., (December & 2008) 1297–1302, ISSN 1062-8738.

Koch, M.E.; Kuen, A.W. & Case, W.E. (1990). Photon avalanche upconversion laser at 644 nm. Appl. Phys. Lett. 56., (January & 1990) 1083–3, ISSN: 0003-6951.

Kurien, K. V. & Ittyachen, M. A. (1979). Growth kinetics and habit modification of barium molybdate single crystals in silica gel. *J. Cryst. Growth.* 47., 5-6., (November-December & 1979) 743-745, , ISSN: 0022-0248.

Li, G.; Zhiping, Y.; Xu, L.; Chong, L. & Panlai, L. (2007). Luminescent Properties of Tb^{3+} doped $CaMoO_4$ Phosphor for UV White Light Emitting Diode. *J. Rare Earths*, 25., 7., (April & 2007) 7294 – 296, ISSN: 1002-0721.

Li, Q.; Huang, J. & Chen, D. (2011). A novel red-emitting phosphors $K_2Ba(MoO_4)_2$: Eu^{3+}, Sm^{3+} and improvement of luminescent properties for light emitting diodes. *J. Alloys Compd.* 509., 3., (January & 2011) 1007-1010, ISSN: 0925-838.

Lifshitz, E.; Bashouti, M.; Kloper, V.; Kigel, A.; Eisen, M.S. & Berger, S. (2003). Synthesis and Characterization of PbSe Quantum Wires, Multipods, Quantum Rods, and Cubes *Nano Lett.* 3., 6., (May & 2003) 857-862, ISSN: 1530-6984.

Lu, W.; Cheng, L.; Zhong, H.; Sun, J.; Wan, J.; Tian, Y. & Chen, B. (2010). Dependence of upconversion emission intensity on Yb^{3+} concentration in Er^{3+}/Yb^{3+} co-doped flake shaped $Y_2(MoO_4)_3$ phosphors *J. Phys. D: Appl. Phys.* 43., 8., (February & 2010) 085404, ISSN: 0022-3727.

Luo, Z.; Li, H.; Shu, H.; Wang, K.; Xia, J. & Yan, Y. (2008). Synthesis of $BaMoO_4$ Nestlike Nanostructures Under a New Growth Mechanism. *Cryst. Growth. Des.* 8., 7., (July & 2008) 2275–2281, ISSN: 1528-7483.

Mao, C-J.; Geng, J.; Wu, X-C. & Zhu, J-J.; (2010). Selective Synthesis and Luminescence Properties of Self-Assembled $SrMoO_4$ Superstructures via a Facile Sonochemical Route. J. Phys. Chem. C. 114., 5., (January & 2010) 1982 – 1988, ISSN: 1932-7447.

Marques, A. P. A.: Longo, V. M.; Melo, D. M.A.; Pizani, P. S.; Leite, E. R.; Varela, J. A. & Longo, E. (2008). Shape controlled synthesis of $CaMoO_4$ thin films and their photoluminescence property. *J. Solid State Chem.* 181., 5., (May & 2008) 1249– 1257, ISSN: 0022-4596.

Marques, A.P.A.; Melo, D.M.A.; Paskocimas, C.A.; Pizani, P.S.; Joya, M.R.; Leite, E.R. & Longo, E. (2006). Photoluminescent $BaMoO_4$ nanopowders prepared by complex polymerization method (CPM). *J. Solid State Chem.* 179., 3., (March & 2006) 671–678, ISSN: 0022-4596.

Moulder, J. F.; Stickle, W. F.; Sobol P. E. & Bomben, K. D. (1992). Handbook of X-Ray Photoelectron Spectroscopy, J. Chastain, (Ed.), 1-254, Perkin-Elmer Corporation, ISBN: 0-9627026-2-5, Eden Prairie, Minnesota, United States of America.

Palai, R.; Choudhary, RN.R. & Sharma, S. (2001). Ferroelectric phase transition in Ni-doped lead molybdate ceramics.*Ferroelectrics*, 256., 1., (April & 2006) 33–45, ISSN: 0015-0193.

Panchal, V.; Garg, N. & Sharma S. M. (2006). Raman and x-ray diffraction investigations on $BaMoO_4$ under high pressures *J. Phys.: Condens. Matter* 18., 16., (April & 2006) 3917, ISSN: 0953-8984.

Peng, X. (2003). Mechanisms for the Shape-Control and Shape-Evolution of Colloidal Semiconductor Nanocrystals. *Adv. Mater.* 15., 459, (March & 2003) ISSN: 1521-4095.

Rosa, I. L. V.; Marques, A. P. A.; Tanaka, M. T. S.; Motta, F. V.; Varela, J. A.; Leite, E. R. & Longo, E. (2009). Europium(III) Concentration Effect on the Spectroscopic and Photoluminescent Properties of BaMoO4:Eu. *J. Fluoresc.* 19., 3., (November & 2008) 495 – 500, ISSN: 1053-0509.

Ryu, J. H.; Yoon, J. W.; Lim, C. S.; Oh, W. C. & Shim, K. B. (2005a). Microwave-assisted synthesis of $CaMoO_4$ nano-powders by a citrate complex method and its photoluminescence property. *J. Alloys Compd.* 390., 1-2., (March & 2005) 245–249, ISSN: 0925-838.

Ryu, J.H.; Yoon, J.W.; Lim, C.S. & Shim, K.B. (2005b). Microwave-assisted synthesis of barium molybdate by a citrate complex method and oriented aggregation. *Mater. Res. Bull.* 40., 9., (September & 2005) 1468 – 1476.

Sen, A. & Pramanik, P. (2001). Low-temperature synthesis of nano-sized metal molybdate powders. *Mater. Lett.* 50.,5-6., (September & 2001) 287-294, ISSN: 0167-577X.

Sivakumar, V. & Varadaraju, U. V. (2006). Intense Red Phosphor for White LEDs Based on Blue GaN LEDs. *J. Electrochem. Soc.*, 153., 3., (February & 2006) H54-H57, ISSN: 0013-4651.

Thongtem, T.; Kungwankunakorn, S.; Kuntalue, B.; Phuruangrat, A. & Thongtern, S. (2010). Luminescence and absorbance of highly crystalline $CaMoO_4$, $SrMoO_4$, $CaWO_4$ and $SrWO_4$ nanoparticles synthesized by co-precipitation method at room temperature. *J. Alloys Compd.* 506., 1., (September & 2010) 475 – 481, ISSN: 0925-838.

Wang, J. G.; Jing, X. P.; Yan, C. H. & Lin, J. H. (2005). $Ca_{1-2x}Eu_xLi_x$ MoO_4: A novel red phosphor for solid-state lighting based on a GaN LED. *J. Electrochem. Soc.*, 152., 3., (January & 2005) G186, ISSN: 0013-4651.

Wang, Y.; Ma, J.; Tao, J.; Zhu, X.; Zhou, J.; Zhao, Z.; Xie, L.; Tian, H. (2007). Low temperature synthesis of $CaMoO_4$ nanoparticles. *Ceram. Int.* 33., 4., (May & 2007) 693 – 695.

Wang, Z.; Liang, H.; Wang, J.; Gong, M. & Su, Q. (2006). Red-light-emitting diodes fabricated by near-ultraviolet InGaN chips with molybdate phosphors. *Appl. Phys. Lett.* 89., 7., (August & 2006) 071921, ISSN: 0003-6951.

Wu, X.; Du, J.; Li, H.; Zhang, M.; Xi, B.; Fan, H.; Zhu, Y. & Qian, Y. (2007). Aqueous mineralization process to synthesize uniform shuttle-like $BaMoO_4$ microcrystals at room temperature. *J. Solid State Chem.* 180., 11., (November & 2007) 3288 – 3295, ISSN: 0022-4596.

Xia, C-T. & Fuenzalida, V.M. (2003). Room temperature electrochemical growth of polycrystalline $BaMoO_4$ films. *J. Euro. Ceram. Soc.* 23., 3., (March & 2003) 519 – 525, ISSN: 0955-2219.

Xie, A.; Yuan, X.; Wang, F.; Shi, Y. & Mu, Z. (2010). Enhanced red emission in $ZnMoO_4$: Eu^{3+} by charge compensation. *J. Phys. D: Appl. Phys.* 43., 5., (January & 2010) 055101, ISSN: 0022-3727.

Xu, L.; Lu, C.; Zhang, Z.; Yang, X. & Hou, W. (2010). Various self-assembled three-dimensional hierarchical architectures of $La_2(MoO_4)_3$: controlled synthesis, growth mechanisms, luminescence properties and adsorption activities. *Nanoscale*, 2., (May & 2010) 995–1005, ISSN: 2040-3364.

Xu, L.; Zhiping, Y.; Li, G.; Qinglin, G.; Sufang, H. & Panlai, L. (2007). Synthesis and Properties of Eu^{3+} Activated Strontium Molybdate Phosphor. *J. Rare Earths.* 25, 6., (December & 2007) 706-709, ISSN: 1002-0721.

Yang, X.Y. ; Liu, J.; Yang, H.; Yu, X.B.; Guo, Y.Z.; Zhou, Y.Q. & Liu, J. (2009). Synthesis and characterization of new red phosphors for white LED applications. *J. Mater. Chem.* 19., 22., (April & 2009) 3771–3774, ISSN: 0959-9428.

Yang, X.Y.; Liu, J.; Yang, H.; Yu, X.B.; Guo, Y.Z.; Zhou, Y.Q. & Liu, J. (2009). Synthesis and characterization of new red phosphors for white LED applications. *J. Mater. Chem.* 19., 22., (April & 2009)3771-3774, ISSN: 0959-9428.

Zhang, G.; Yu, S.; Yang, Y.; Jiang, W.; Zhang, S. & Huang, B. (2010) . Synthesis, morphology and phase transition of the zinc molybdates $ZnMoO_4 \cdot 0.8H_2O$/α-$ZnMoO_4$/$ZnMoO_4$

by hydrothermal method. *J. Crystal Growth.* 312., 11., (May 2010) 1866–1874, ISSN: 0022-0248.

Zhang, N.; Bu, W.; Xu, Y.; Jiang, D. & Shi, J. (2007). Self-Assembled Flowerlike Europium-Doped Lanthanide Molybdate Microarchitectures and Their Photoluminescence Properties. *J. Phys. Chem. C.* 111, 5014 – 5019, ISSN: 1932-7447.

Zhang, Y.; Yang, F.; Yang, J.; Tang, Y. & Yuan, P. (2005) Synthesis of crystalline $SrMoO_4$ nanowires from polyoxometalates. *Solid State Commun.* 133., 12., (March & 2005) 759 – 763.

Materials Science and Technology
Edited by Prof. Sabar Hutagalung

ISBN 978-953-51-0193-2
Hard cover, 324 pages
Publisher InTech
Published online 07, March, 2012
Published in print edition March, 2012

Materials are important to mankind because of the benefits that can be derived from the manipulation of their properties, for example electrical conductivity, dielectric constant, magnetization, optical transmittance, strength and toughness. Materials science is a broad field and can be considered to be an interdisciplinary area. Included within it are the studies of the structure and properties of any material, the creation of new types of materials, and the manipulation of a material's properties to suit the needs of a specific application. The contributors of the chapters in this book have various areas of expertise. therefore this book is interdisciplinary and is written for readers with backgrounds in physical science. The book consists of fourteen chapters that have been divided into four sections. Section one includes five chapters on advanced materials and processing. Section two includes two chapters on bio-materials which deal with the preparation and modification of new types of bio-materials. Section three consists of three chapters on nanomaterials, specifically the study of carbon nanotubes, nano-machining, and nanoparticles. Section four includes four chapters on optical materials.

InTech Europe
University Campus STeP Ri
Slavka Krautzeka 83/A
51000 Rijeka, Croatia
Phone: +385 (51) 770 447
Fax: +385 (51) 686 166
www.intechopen.com

InTech China
Unit 405, Office Block, Hotel Equatorial Shanghai
No.65, Yan An Road (West), Shanghai, 200040, China
中国上海市延安西路65号上海国际贵都大饭店办公楼405单元
Phone: +86-21-62489820
Fax: +86-21-62489821

IntechOpen